PROCEEDINGS OF SCIENCE

The Real-Time Analysis Platform of KM3NeT and its first results

S. Celli[a,b,*] **and P. Demin, D. Dornic, F. Filippini, E. Giorgio, E. Le Guirriec, J. De Favereau de Jeneret, M. Lamoureux, M. Mastrodicasa, J. Palacios Gonzalez, S. Le Stum, J. Tanasijczuk, G. Vannoye, A. Veutro, A. Zegarelli for the KM3NeT Collaboration**

[a] *Sapienza Università di Roma, Piazzale Aldo Moro 5, 00185, Rome, Italy*

[b] *Istituto Nazionale di Fisica Nucleare, Sezione di Roma, Piazzale Aldo Moro 5, 00185, Rome, Italy*

E-mail: silvia.celli@roma1.infn.it

KM3NeT is a multi-site neutrino telescope under construction in the depth of the Mediterranean Sea, consisting of two Cherenkov telescopes, ARCA and ORCA, both of which are currently in data-taking. Among the primary scientific goals of KM3NeT are the observation of cosmic neutrinos and the investigation of their sources. ARCA and ORCA are optimized in complementary energy ranges, allowing for the exploration of neutrino astronomy from MeV to tens of PeV. The combination of an extended field of view and a high duty cycle of Cherenkov-based neutrino detectors is crucial for detecting and informing other telescopes about interesting neutrino candidates in a very short time. As emission from these sources can rapidly fade, the alerts need to be shared with low latency, in order to allow for a prompt follow-up in the multi-messenger and multi-wavelength domains, particularly for the detection of transient and variable sources. In the case of poorly localized triggers, such as gravitational waves, KM3NeT can provide refined pointing directions, representing a further advantage. This contribution reports on the status of the software architecture implemented in KM3NeT for a fast reconstruction and classification of events occurring in the detectors. Additionally, the results of the online processing of KM3NeT data in coincidence with GRB221009A will be presented.

38th International Cosmic Ray Conference (ICRC2023)
26 July - 3 August, 2023
Nagoya, Japan

ICRC2023 38th International Cosmic Ray Conference The Astroparticle Physics Conference

*Speaker

PoS(ICRC2023)1125

1. Introduction

The goal of real-time alert systems is to enable multi-messenger (MM) observations allowing the localization and identification of sources, particularly in the presence of fading events. Thanks to its fast response, almost continuous duty cycle, and large field of view, KM3NeT is well suited to trigger observatories with limited solid angle visibility to quickly point their instruments in a well-defined direction of the sky. Other way around, KM3NeT can carry out follow-up observations of external triggers, thus enhancing the utility of joint observation campaigns. The rapid provision of alerts is crucial to detect transient and variable sources, such that fast algorithms coupled with automated notification systems have to be employed in the online processing of events.
The KM3NeT Collaboration has developed a Real-Time Analysis (RTA) platform for each of its two detectors: after validation in a six-month commissioning period, the system is currently implemented into the standard data flow. It is now regularly reconstructing and classifying events with a median latency below ~ 10 s for both ARCA and ORCA data, as well as receiving and processing external alerts. The recent start of the fourth data taking run of the two LIGO Gravitational-Wave (GW) interferometers is hence accompanied by the KM3NeT monitoring of the neutrino sky, in analogy with the MM activities performed during the previous acquisition run of LIGO-Virgo [1]. This contribution describes the status of the RTA framework implemented in KM3NeT. In Sec. 2 the main features of the experimental apparatus are described, followed in Sec. 3 by details of the framework that has been developed for the real-time trigger and follow-up of MM alerts. This section also reports on the online analysis of GRB221009A, the most luminous Gamma-Ray Burst (GRB) ever detected, which occurred during the commissioning of the KM3NeT RTA system. Conclusions are drawn in Sec. 4.

2. KM3NeT

KM3NeT [2] is an European research infrastructure consisting of a network of deep-sea neutrino detectors located in the Mediterranean Sea: ARCA offshore Sicily (Italy) at 3.5 km depth, and ORCA offshore Toulon (France) at 2.5 km depth. These are three dimensional arrays of photo-sensors recording the time, position and charge deposit of Cherenkov hits induced by the passage in water of ultra-relativistic charged particles produced at neutrino interactions, thus allowing for the reconstruction of the incoming neutrino direction and energy. The two instruments profit of the same technology, based on the Digital Optical Modules (DOMs), glass spheres hosting 31 3″ Photo-Multiplier Tubes (PMTs) as well as the electronics for data acquisition and calibration [3]. 18 DOMs compose a Detection Unit (DU). At the time of writing, the two detectors are taking data, ARCA with 21 DUs and ORCA with 18 DUs, in the so-called ARCA21 and ORCA18 configurations, respectively. Besides the different location and depth, ARCA is the larger and more sparsely instrumented detector compared to ORCA. In ARCA, the DUs are horizontally separated from each other by an average distance of about 90 m and the vertical distance between DOMs belonging to the same DU is 36 m. In contrast, the DUs in ORCA are installed about 20 m apart and the vertical distance between DOMs is 9 m. The different geometries of ARCA and ORCA permit scientists to explore complementary energy ranges of the interacting neutrinos: ARCA has enhanced sensitivity in the multi-TeV domain, while ORCA is optimized for the detection of sub-TeV

PoS(ICRC2023)1125

neutrinos. Moreover, searches for MeV neutrinos, e.g. those expected in Core Collapse SuperNova (CCSN) explosions, can be performed exploiting signals in individual DOMs, by looking for an increased rate in hit coincidences within its PMTs. The broad energy coverage of the two KM3NeT detectors hence enables analyses in the MeV to multi-PeV domain. In addition, the high duty cycle of Cherenkov detectors, coupled to the 4π field of view, guarantees continuous monitoring of the neutrino sky, which is of paramount importance in the context of transient and variable emissions from cosmic sources. To fully explore the time-domain neutrino astronomy, the KM3NeT Collaboration has implemented a real-time reconstruction and classification system of events, allowing for a fast selection of a high-purity neutrino sample as well as for follow up external triggers. The KM3NeT RTA system is described in the following, with a focus on the latency times for event processing and alert distribution to the external community.

3. The RTA framework

The KM3NeT telescopes follow the so-called *all data-to-shore* concept, i.e. all data are sent from the detectors to their respective control stations on the shores, where the Data Acquisition System (DAQ) applies an automated filtering in order to reduce the data output for storage. Before data writing, the collected hits and triggered events are propagated into the RTA platform, where they are sudden processed through different pipelines. Two RTA modules are running continuously in the detector shore stations, in order to identify interesting neutrino-induced events within KM3NeT data. One is the online processing pipeline for reconstruction and classification of events induced by the interaction of GeV-PeV neutrinos; the other is the MeV SN analysis, as detailed in Sec. 3.1. Data from each detector are then transferred to a common dispatcher, where analysis pipelines are activated: these include both auto-correlation searches as well as follow-up studies, starting automatically whenever an interesting external alert is received from the MM community. Currently, four follow-up analyses are in place, looking for space and time coincidences between KM3NeT events and GWs, GRBs, other transients and high-energy neutrinos from IceCube, as presented in Sec. 3.2. The described data flow is schematically illustrated in Fig. 1.

3.1 The online GeV-PeV event processing module

Neutrinos with energies in the GeV-PeV range can trigger multiple DOMs in the detector, leaving two distinct topological signatures according to their flavor and interaction channels, namely: 1) track-like events, mainly from the charged-current (CC) interactions of muon neutrinos ν_μ and partially from the CC interactions of tau neutrinos ν_τ; 2) shower-like events, from the electron neutrino ν_e CC interactions, the neutral-current (NC) interactions of all neutrino flavors and the majority of tau neutrino CC interactions. Based on these two event signatures, KM3NeT reconstruction algorithms can be divided into track and shower reconstructions [4], the former providing the best angular resolution and the latter featuring a remarkable energy resolution, particularly for contained events. Both the online directional and energy reconstruction adopt the same algorithms as in offline, with the exception that some steps are avoided in the online chain in order to process data as fast as possible. A further difference among online and offline reconstructions is the fact that dynamical calibrations are not yet implemented in the real-time chain: while optimizations are in progress, the current track-like reconstruction of ARCA21 data can achieve sub-degree precision

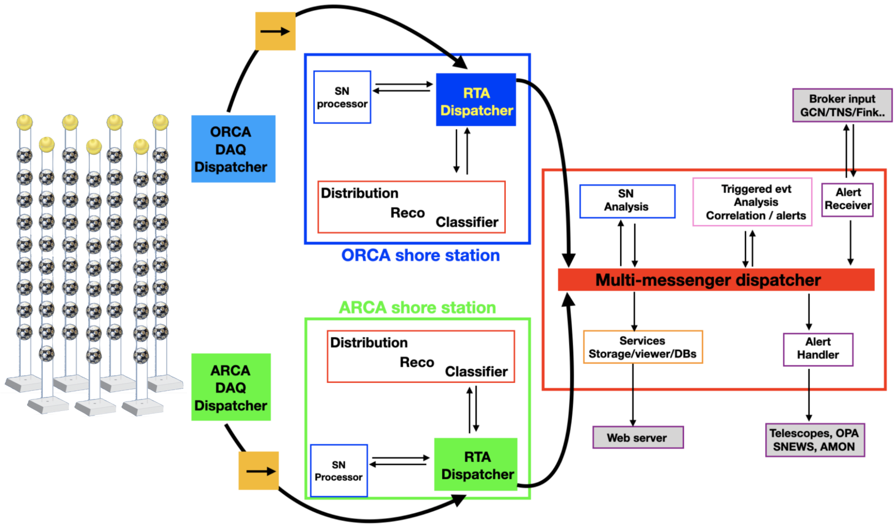

Figure 1: A schematic illustration of the real-time framework architecture of KM3NeT.

for neutrino energies above 10 TeV [5].
To handle the high trigger rate with low latency, parallel multi-core processing is adopted: Fig. 2 shows the rate of reconstructed events in a time window of few days with the detector configurations ARCA21 and ORCA18. For the same event topology, the rate of reconstructed events is different for the two detectors because of the different depth where they are located, the deeper location of ARCA implying a lower background from atmospheric muons.

The event processing at the ARCA and ORCA shore stations is implemented through different architectures: for each ARCA event, topological reconstructions and classifications are run in parallel, while ORCA data are processed serially, namely a single client is in charge for both the track-like, the shower-like and the classification of an individual triggered event. Fig. 3 shows histograms of the resulting online processing times of individual events, in the two current detector configurations: in the case of ARCA21, a median delay of 3.6 s is achieved between the event triggering and its reconstruction by either the track-like or the shower-like algorithm (hence including the data filtering from background noise, its buffering, dispatching and finally reconstruction times), as visible in Figs. 3(a) and 3(b), respectively. An analogous timescale is obtained in the classification processing, as shown in Fig. 3(c), where the time shown includes again filtering, buffering, and dispatching of data before the actual classification. A median of 6.0 s is achieved for ORCA18 events, such a delay including filtering, buffering, dispatching, serial topological reconstruction and classification, as shown in Fig. 3(d).
With regards to the classification algorithms that are currently in place for both ARCA and ORCA, machine learning techniques are being adopted, both Boosted Decision Trees and Graph Neural Networks capable of fully exploiting the detector geometry. A first classifier aims at performing a fast neutrino classification to separate neutrinos from the large muon background: each event is evaluated with a classification score indicating the probability of it being a neutrino, its output being crucial in the process of neutrino selection in the following correlation search module. A second classifier, in turns, determines the most likely event topology, providing the likelihood for the event

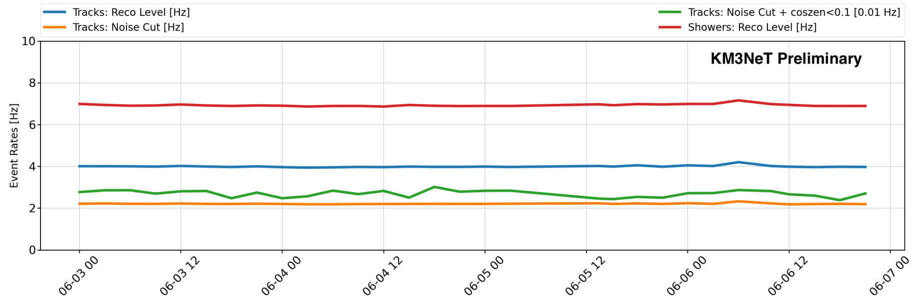

(a)

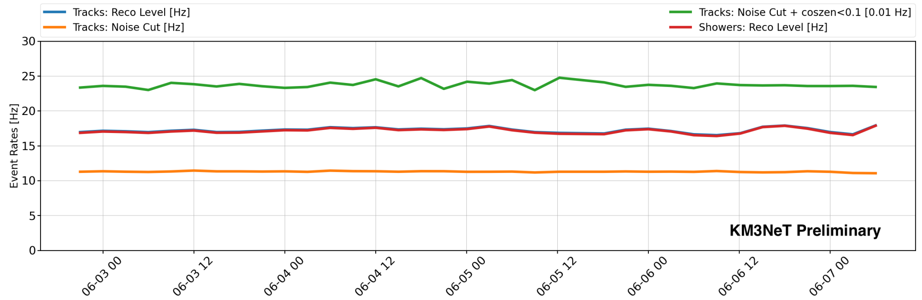

(b)

Figure 2: Event rate at (online) reconstruction level in ARCA21 (a) and ORCA18 (b) as a function of time, from June 03rd to June 07th 2023.

to belong to either the track or the shower sample. Currently, the processing time taken by each classifier amounts to $\sim$ 0.3 s/event. After the event classification, ARCA and ORCA data streams are combined for common analysis and any subsequent alerts in the so-called MM dispatcher, shown in Fig. 1. At this level, a neutrino sample can be selected by choosing the appropriate cut on the classification scores depending on the analysis.

3.2 The MeV neutrino CCSN module

The main goal of the MeV CCSN pipeline is to provide early warning for optical telescopes for the observation of the next Galactic CCSN, as SN neutrinos arrive hours before the electromagnetic signals [6]. The KM3NeT real-time SN analysis takes as input the raw PMT data, such that each DOM acts as a standalone detector and coincidences among its PMT hits are investigated [7, 8]. The number of PMTs hit in a coincidence is defined as the *multiplicity*: the KM3NeT CCSN pipeline evaluates the multiplicity every 0.1 s in a 0.5 s sliding window, where the size of the window corresponds to the typical duration of the accretion phase of the $\bar{\nu}_e$ burst. Radioactive decays dominate at low multiplicities, while the contribution of atmospheric muons dominates above a multiplicity of 8. The latter background can be reduced by exploiting the fact that muon tracks typically produce correlated coincidences on multiple DOMs: as shown in Fig. 4(a), such a filtering permits ORCA to achieve lower background values than ARCA, thanks to the fact that the denser array can more efficiently identify low-energy atmospheric events. The same figure shows the expected event rates from simulated CCSN bursts, which increase with the mass of the progenitor's

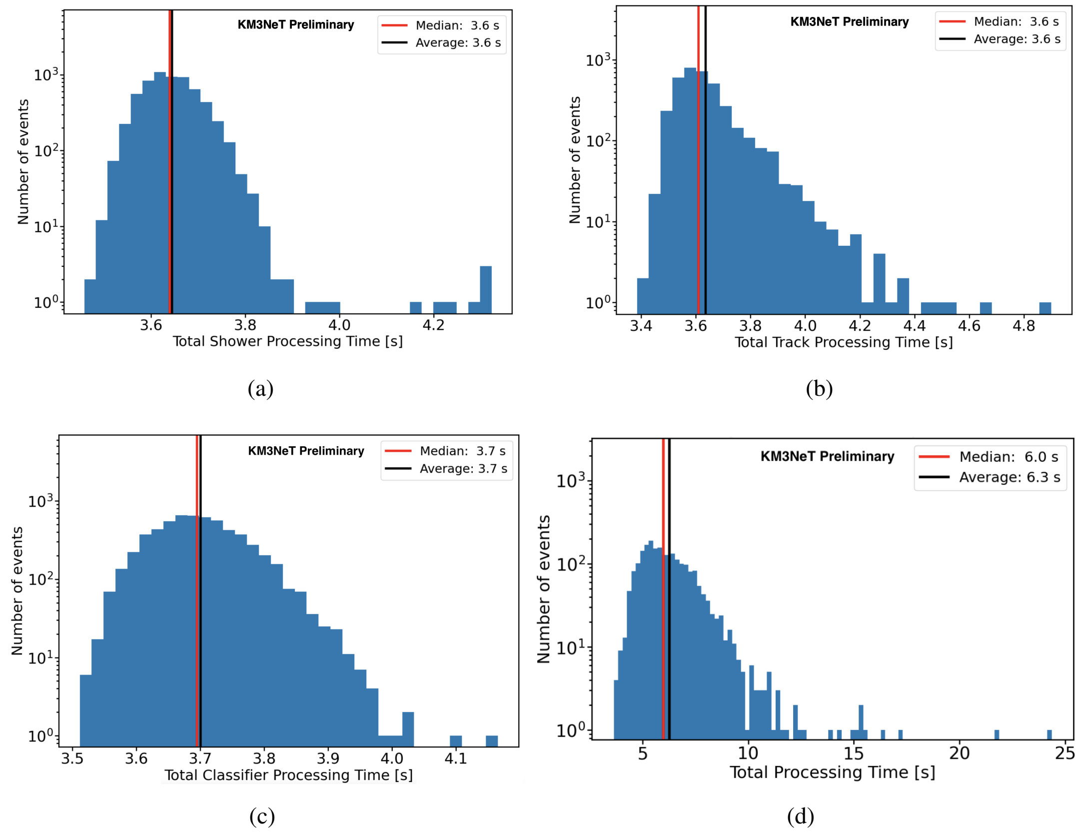

Figure 3: ARCA21 real-time processing times for event acquisition, distribution, reconstruction into track-like (a) and shower-like (b) topologies, and classification (c). (d) ORCA18 real-time processing times for event acquisition, distribution, reconstruction into both track-like and shower-like topologies, and classification.

star. The simulations indicate that the KM3NeT sensitivity is maximal at high multiplicities and that more than 95% of the Galactic CCSNe are potentially observable, in the scenario with progenitor's mass of 11 $M_\odot$ and above. The KM3NeT MeV neutrino CCSN module is operational, and it is sending alerts with false alarm rate less than 1/week to SNEWS [9] with a latency shorter than 20 s.

3.3 Analysis pipelines for multi-messenger alert follow-up

At the reception of an external alert, analysis pipelines are triggered simultaneously both for ARCA and ORCA accordingly to the type of alert, namely a parser reads the incoming message and extracts relevant information to run the corresponding analysis pipeline [10]. A preliminary alert selection is performed at this stage, based on source visibility, quoted size of error box, time delay between event trigger and alert reception, and false alarm rate of the notice.
Currently, four kinds of real-time analyses are in place to look for temporal and spatial coincidences among the KM3NeT reconstructed events and either: i) GRBs, ii) GW extended region, iii) neutrinos identified by IceCube, and iv) transient events (e.g. flaring/variable objects). In addition to these, a pipeline for MeV neutrinos in coincidence with GWs is also in place, that similarly to the SN analysis counts the number of coincidences within single DOMs in a sliding window of 0.5 s.
Each analysis pipeline implements its own search strategy (upgoing/downgoing), gets the recon-

structed events, applies the predefined event selection for track and shower events, performs the correlation search and produces the results, merging both event channels. Different iterations of the pipeline are performed with progressively extended time windows, possibly including the most refined coordinates of the alert. For the MeV neutrino analysis, the time window starts at the time of the alert $t_{\rm alert}$ with a width of 2 seconds afterwards. For the high-energy event search in coincidence with GWs, two iterations are run, the first from $t_{\rm alert} - 500$ s to $t_{\rm alert} + 500$ s, and the second up to 6 hours after the alert. Also for neutrinos two iterations are performed, but in different time windows, respectively $[t_{\rm alert} - 1\ {\rm h}; t_{\rm alert} + 1\ {\rm h}]$ and $[t_{\rm alert} - 24\ {\rm h}; t_{\rm alert} + 24\ {\rm h}]$. For GRBs and all other transients, in turn, four iterations are run, the first in the time window $[t_{\rm alert} - 24\ {\rm h}; t_{\rm alert}]$, and the following up to 3 hr, 6 hr and 24 hr. The expected background is estimated using a few days before the alert.

3.3.1 The online follow-up of GRB221009A

On 2022 October 9th, the brightest GRB ever recorded triggered the gamma-ray instruments onboard of the Swift and Fermi satellites. At first, Swift-BAT reported a transient event at 14:10:17 UT, first cataloged as Swift J1913.1+1946 [11], at RA = 288.263°, DEC = +19.803°. Fermi-GBM triggered an event at 13:16:59 UT at a location consistent with Swift-BAT [12]. Later, LHAASO reported the observation of GRB221009A [13] with energy above 500 GeV by the LHAASO-WCDA (within 2000 seconds after T0) and with energy up to ~ 10 TeV with LHAASO-KM2A, the highest energy radiation ever detected from GRBs. IceCube soon performed a search for track-like muon neutrino events, at first in a time window of -1 hour/+2 hours from the initial trigger reported by Fermi-GBM, and later in a time window of 2 days [14]. In both cases, data were consistent with background only expectations, which allowed for setting upper limits on the time-integrated muon-neutrino flux set respectively at $E^2 dN/dE = 3.9 \times 10^{-2}$ GeV cm^{-2} for the first search and 4.1×10^{-2} GeV cm^{-2} at 90% CL (assuming an E^{-2} power law for the neutrino spectrum).

A quick follow-up was also performed using KM3NeT online data: unfortunately, at the time of the alert, the source was above the KM3NeT horizon, as shown by the sky map in Fig. 4(b). The search for MeV neutrinos yielded a result compatible with background expectations. In addition, two high-energy analyses were run, based on an on/off technique: for ARCA, a region of interest radius of 2° was used; for ORCA, an angular search radius of 4° was adopted instead, the larger size being related to the higher kinematics angle between the parent neutrino and the emerging muon at low energies. No events were found in the on region of any of the online analyses, whose results have been published in [15]; a refined follow up analysis was also performed, confirming the lack of associated neutrinos in KM3NeT data, as reported in [16].

4. Conclusions

The construction and data taking of the KM3NeT infrastructure is ongoing at two designated sites, where the ARCA and ORCA telescopes are located. Each detector currently implements a real-time alert system, capable of fast reconstruction and classification of neutrino-induced events as well as of prompt correlation analyses in response to MM external alerts. A specific monitoring system ensures the stability and sanity of all processes involved in the RTA framework, supported by dedicated shift crews. At the time of writing, more than 300 alerts have been selected and

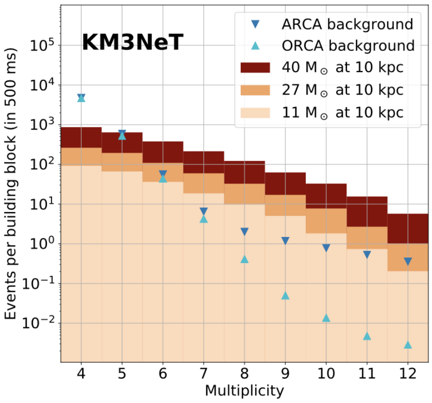

(a)

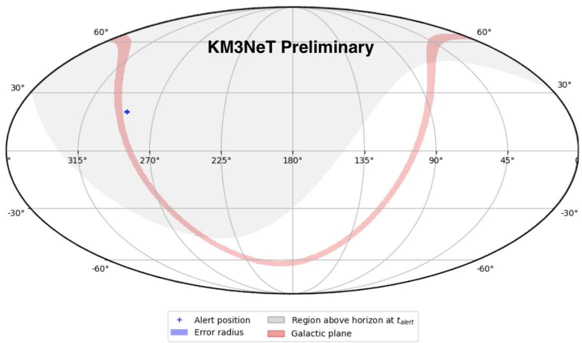

(b)

Figure 4: (a) Expected events in ARCA and ORCA (one BB) from a Galactic SN with different progenitor's mass as a function of multiplicity, compared with background rates. Figure from [6]. (b) Equatorial coordinate sky map showing the position of GRB221009A at its occurrence and the KM3NeT visibility.

processed, of which 191 with GRBs, 119 in coincidence with GW candidates, 50 with neutrinos, and 13 with other transients. A summary of these activities can be found at [10].

References

[1] M. Lamoureux et al. [KM3NeT Coll.], *PoS*(ICRC2023) **1506** (2023);

[2] S. Adrian-Martinez et al. [KM3NeT Coll.], *J. Phys. G: Nuclear and Particle Physics* **43** (2016) 8;

[3] S. Aiello et al. [KM3NeT Coll.], *Journal of Instrumentation* **17** (2022) P07038;

[4] K. Melis, A. Heijboer & M. De Jong [KM3NeT Coll.], *PoS* (ICRC2017) **950** (2018);

[5] R. Muller et al. [KM3NeT Coll.], *PoS*(ICRC2023) **10108** (2023);

[6] S. Aiello et al. [KM3NeT Coll.], *Eur. Phys. J. C.* **81** (2021) 445;

[7] S. Aiello et al. [KM3NeT Coll.], *Eur. Phys. J. C* **82** (2022) 317;

[8] G. Vannoye et al. [KM3NeT Coll.], *PoS* (ICRC2023) **1223** (2023);

[9] S. Al Kharusi et al., *New J. Phys.* **23** (2021) 031201;

[10] J. Palacio-Gonzalez et al. [KM3NeT Coll.], *PoS* (ICRC2023) **1521** (2023);

[11] https://astronomerstelegram.org/?read=15650

[12] https://gcn.gsfc.nasa.gov/gcn3/32636.gcn3

[13] https://gcn.gsfc.nasa.gov/gcn3/32677.gcn3

[14] https://gcn.gsfc.nasa.gov/gcn3/32665.gcn3

[15] https://gcn.gsfc.nasa.gov/gcn3/32741.gcn3

[16] J. Palacio-Gonzalez et al. [KM3NeT Coll.], *PoS*(ICRC2023) **1503** (2023).

Full Authors List: The KM3NeT Collaboration

S. Aiello[a], A. Albert[b,bd], S. Alves Garre[c], Z. Aly[d], A. Ambrosone[f,e], F. Ameli[g], M. Andre[h], E. Androutsou[i], M. Anguita[j], L. Aphecetche[k], M. Ardid[l], S. Ardid[l], H. Atmani[m], J. Aublin[n], L. Bailly-Salins[o], Z. Bardačová[q,p], B. Baret[n], A. Bariego-Quintana[c], S. Basegmez du Pree[r], Y. Becherini[n], M. Bendahman[m,n], F. Benfenati[t,s], M. Benhassi[u,e], D. M. Benoit[v], E. Berbee[r], V. Bertin[d], S. Biagi[w], M. Boettcher[x], D. Bonanno[w], J. Boumaaza[m], M. Bouta[y], M. Bouwhuis[r], C. Bozza[z,e], R. M. Bozza[f,e], H.Brânzaş[aa], F. Bretaudeau[k], R. Bruijn[ab,r], J. Brunner[d], R. Bruno[a], E. Buis[ac,r], R. Buompane[u,e], J. Busto[d], B. Caiffi[ad], D. Calvo[c], S. Campion[g,ae], A. Capone[g,ae], F. Carenini[t,s], V. Carretero[c], T. Cartraud[n], P. Castaldi[af,s], V. Cecchini[c], S. Celli[g,ae], L. Cerisy[d], M. Chabab[ag], M. Chadolias[ah], A. Chen[ai], S. Cherubini[aj,w], T. Chiarusi[s], M. Circella[ak], R. Cocimano[w], J. A. B. Coelho[n], A. Coleiro[n], R. Coniglione[w] P. Coyle[d], A. Creusot[n], A. Cruz[al], G. Cuttone[w], R. Dallier[k], Y. Darras[ah], A. De Benedittis[e], B. De Martino[d], V. Decoene[k], R. Del Burgo[e], U. M. Di Cerbo[e], L. S. Di Mauro[w], I. Di Palma[g,ae], A. F. Díaz[j], C. Diaz[j], D. Diego-Tortosa[w], C. Distefano[w], A. Domi[ah], C. Donzaud[n], D. Dornic[d], M. Dörr[am], E. Drakopoulou[i], D. Drouhin[b,bd], R. Dvornický[q], T. Eberl[ah], E. Eckerová[q,p], A. Eddymaoui[m], T. van Eeden[r], M. Eff[n], D. van Eijk[r], I. El Bojaddaini[y], S. El Hedri[n], A. Enzenhöfer[d], G. Ferrara[w], M. D. Filipović[an], F. Filippini[t,s], D. Franciotti[w], L. A. Fusco[z,e], J. Gabriel[ao], S. Gagliardini[g], T. Gal[ah], J. García Méndez[l], A. Garcia Soto[c], C. Gatius Oliver[r], N. Geißelbrecht[ah], H. Ghaddari[y], L. Gialanella[e,u], B. K. Gibson[v], E. Giorgio[w], I. Goos[n], D. Goupilliere[o], S. R. Gozzini[c], R. Gracia[ah], K. Graf[ah], C. Guidi[ap,ad], B. Guillon[o], M. Gutiérrez[aq], H. van Haren[ar], A. Heijboer[r], A. Hekalo[am], L. Hennig[ah], J. J. Hernández-Rey[c], F. Huang[d], W. Idrissi Ibnsalih[e], G. Illuminati[s], C. W. James[al], M. de Jong[as,r], P. de Jong[ab,r], B. J. Jung[r], P. Kalaczyński[at,be], O. Kalekin[ah], U. F. Katz[ah], N. R. Khan Chowdhury[c], A. Khatun[q], G. Kistauri[av,au], C. Kopper[ah], A. Kouchner[aw,n], V. Kulikovskiy[ad], R. Kvatadze[av], M. Labalme[o], R. Lahmann[ah], M. Lamoureux[bf], G. Larosa[w], C. Lastoria[d], A. Lazo[c], E. Le Guirriec[d], S. Le Stum[d], G. Lehaut[o], E. Leonora[a], N. Lessing[c], G. Levi[t,s], M. Lindsey Clark[n], F. Longhitano[a], J. Majumdar[r], L. Malerba[ad], F. Mamedov[p], J. Mańczak[c], A. Manfreda[e], M. Marconi[ap,ad], A. Margiotta[t,s], A. Marinelli[e,f], C. Markou[i], L. Martin[k], J. A. Martínez-Mora[l], F. Marzaioli[u,e], M. Mastrodicasa[ae,g], S. Mastroianni[e], S. Miccichè[w], G. Miele[f,e], P. Migliozzi[e], E. Migneco[w], M. L. Mitsou[e], C. M. Mollo[e], L. Morales-Gallegos[u,e], C. Morley-Wong[al], A. Moussa[y], I. Mozun Mateo[ay,ax], R. Muller[r], M. R. Musone[e,u], M. Musumeci[w], L. Nauta[r], S. Navas[aq], A. Nayerhoda[ak], C. A. Nicolau[g], B. Nkosi[ai], B. Ó Fearraigh[ab,r], V. Oliviero[f,e], A. Orlando[w], E. Oukacha[n], D. Paesani[w], J. Palacios González[c], G. Papalashvili[au], V. Parisi[ap,ad], E.J. Pastor Gomez[c], A. M. Păun[aa], G. E. Păvălaş[aa], S. Peña Martínez[n], M. Perrin-Terrin[d], J. Perronnel[o], V. Pestel[ay], R. Pestes[n], P. Piattelli[w], C. Poirè[z,e], V. Popa[aa], T. Pradier[b], S. Pulvirenti[w], G. Quéméner[o], C. Quiroz[l], U. Rahaman[c], N. Randazzo[a], R. Randriatoamanana[k], S. Razzaque[az], I. C. Rea[e], D. Real[c], S. Reck[ah], G. Riccobene[w], J. Robinson[x], A. Romanov[ap,ad], A. Šaina[c], F. Salesa Greus[c], D. F. E. Samtleben[as,r], A. Sánchez Losa[c,ak], S. Sanfilippo[w], M. Sanguineti[ap,ad], C. Santonastaso[ba,e], D. Santonocito[w], P. Sapienza[w], J. Schnabel[ah], J. Schumann[ah], H. M. Schutte[x], J. Seneca[r], N. Sennan[y], B. Setter[ah], I. Sgura[ak], R. Shanidze[au], Y. Shitov[p], F. Šimkovic[q], A. Simonelli[e], A. Sinopoulou[a], M.V. Smirnov[ah], B. Spisso[e], M. Spurio[t,s], D. Stavropoulos[i], I. Štekl[p], M. Taiuti[ap,ad], Y. Tayalati[m], H. Tedjditi[ad], H. Thiersen[x], I. Tosta e Melo[a,aj], B. Trocmé[n], V. Tsourapis[i], E. Tzamariudaki[i], A. Vacheret[o], V. Valsecchi[w], V. Van Elewyck[aw,n], G. Vannoye[d], G. Vasileiadis[bb], F. Vazquez de Sola[r], C. Verilhac[n], A. Veutro[g,ae], S. Viola[w], D. Vivolo[u,e], J. Wilms[bc], E. de Wolf[ab,r], H. Yepes-Ramirez[l], G. Zarpapis[i], S. Zavatarelli[ad], A. Zegarelli[g,ae], D. Zito[w], J. D. Zornoza[c], J. Zúñiga[c], and N. Zywucka[x].

[a] INFN, Sezione di Catania, Via Santa Sofia 64, Catania, 95123 Italy
[b] Université de Strasbourg, CNRS, IPHC UMR 7178, F-67000 Strasbourg, France
[c] IFIC - Instituto de Física Corpuscular (CSIC - Universitat de València), c/Catedrático José Beltrán, 2, 46980 Paterna, Valencia, Spain
[d] Aix Marseille Univ, CNRS/IN2P3, CPPM, Marseille, France
[e] INFN, Sezione di Napoli, Complesso Universitario di Monte S. Angelo, Via Cintia ed. G, Napoli, 80126 Italy
[f] Università di Napoli "Federico II", Dip. Scienze Fisiche "E. Pancini", Complesso Universitario di Monte S. Angelo, Via Cintia ed. G, Napoli, 80126 Italy
[g] INFN, Sezione di Roma, Piazzale Aldo Moro 2, Roma, 00185 Italy
[h] Universitat Politècnica de Catalunya, Laboratori d'Aplicacions Bioacústiques, Centre Tecnològic de Vilanova i la Geltrú, Avda. Rambla Exposició, s/n, Vilanova i la Geltrú, 08800 Spain
[i] NCSR Demokritos, Institute of Nuclear and Particle Physics, Ag. Paraskevi Attikis, Athens, 15310 Greece
[j] University of Granada, Dept. of Computer Architecture and Technology/CITIC, 18071 Granada, Spain
[k] Subatech, IMT Atlantique, IN2P3-CNRS, Université de Nantes, 4 rue Alfred Kastler - La Chantrerie, Nantes, BP 20722 44307 France
[l] Universitat Politècnica de València, Instituto de Investigación para la Gestión Integrada de las Zonas Costeras, C/ Paranimf, 1, Gandia, 46730 Spain
[m] University Mohammed V in Rabat, Faculty of Sciences, 4 av. Ibn Battouta, B.P. 1014, R.P. 10000 Rabat, Morocco
[n] Université Paris Cité, CNRS, Astroparticule et Cosmologie, F-75013 Paris, France
[o] LPC CAEN, Normandie Univ, ENSICAEN, UNICAEN, CNRS/IN2P3, 6 boulevard Maréchal Juin, Caen, 14050 France
[p] Czech Technical University in Prague, Institute of Experimental and Applied Physics, Husova 240/5, Prague, 110 00 Czech Republic
[q] Comenius University in Bratislava, Department of Nuclear Physics and Biophysics, Mlynska dolina F1, Bratislava, 842 48 Slovak Republic
[r] Nikhef, National Institute for Subatomic Physics, PO Box 41882, Amsterdam, 1009 DB Netherlands
[s] INFN, Sezione di Bologna, v.le C. Berti-Pichat, 6/2, Bologna, 40127 Italy
[t] Università di Bologna, Dipartimento di Fisica e Astronomia, v.le C. Berti-Pichat, 6/2, Bologna, 40127 Italy
[u] Università degli Studi della Campania "Luigi Vanvitelli", Dipartimento di Matematica e Fisica, viale Lincoln 5, Caserta, 81100 Italy
[v] E. A. Milne Centre for Astrophysics, University of Hull, Hull, HU6 7RX, United Kingdom

[w] INFN, Laboratori Nazionali del Sud, Via S. Sofia 62, Catania, 95123 Italy
[x] North-West University, Centre for Space Research, Private Bag X6001, Potchefstroom, 2520 South Africa
[y] University Mohammed I, Faculty of Sciences, BV Mohammed VI, B.P. 717, R.P. 60000 Oujda, Morocco
[z] Università di Salerno e INFN Gruppo Collegato di Salerno, Dipartimento di Fisica, Via Giovanni Paolo II 132, Fisciano, 84084 Italy
[aa] ISS, Atomistilor 409, Măgurele, RO-077125 Romania
[ab] University of Amsterdam, Institute of Physics/IHEF, PO Box 94216, Amsterdam, 1090 GE Netherlands
[ac] TNO, Technical Sciences, PO Box 155, Delft, 2600 AD Netherlands
[ad] INFN, Sezione di Genova, Via Dodecaneso 33, Genova, 16146 Italy
[ae] Università La Sapienza, Dipartimento di Fisica, Piazzale Aldo Moro 2, Roma, 00185 Italy
[af] Università di Bologna, Dipartimento di Ingegneria dell'Energia Elettrica e dell'Informazione "Guglielmo Marconi", Via dell'Università 50, Cesena, 47521 Italia
[ag] Cadi Ayyad University, Physics Department, Faculty of Science Semlalia, Av. My Abdellah, P.O.B. 2390, Marrakech, 40000 Morocco
[ah] Friedrich-Alexander-Universität Erlangen-Nürnberg (FAU), Erlangen Centre for Astroparticle Physics, Nikolaus-Fiebiger-Straße 2, 91058 Erlangen, Germany
[ai] University of the Witwatersrand, School of Physics, Private Bag 3, Johannesburg, Wits 2050 South Africa
[aj] Università di Catania, Dipartimento di Fisica e Astronomia "Ettore Majorana", Via Santa Sofia 64, Catania, 95123 Italy
[ak] INFN, Sezione di Bari, via Orabona, 4, Bari, 70125 Italy
[al] International Centre for Radio Astronomy Research, Curtin University, Bentley, WA 6102, Australia
[am] University Würzburg, Emil-Fischer-Straße 31, Würzburg, 97074 Germany
[an] Western Sydney University, School of Computing, Engineering and Mathematics, Locked Bag 1797, Penrith, NSW 2751 Australia
[ao] IN2P3, LPC, Campus des Cézeaux 24, avenue des Landais BP 80026, Aubière Cedex, 63171 France
[ap] Università di Genova, Via Dodecaneso 33, Genova, 16146 Italy
[aq] University of Granada, Dpto. de Física Teórica y del Cosmos & C.A.F.P.E., 18071 Granada, Spain
[ar] NIOZ (Royal Netherlands Institute for Sea Research), PO Box 59, Den Burg, Texel, 1790 AB, the Netherlands
[as] Leiden University, Leiden Institute of Physics, PO Box 9504, Leiden, 2300 RA Netherlands
[at] National Centre for Nuclear Research, 02-093 Warsaw, Poland
[au] Tbilisi State University, Department of Physics, 3, Chavchavadze Ave., Tbilisi, 0179 Georgia
[av] The University of Georgia, Institute of Physics, Kostava str. 77, Tbilisi, 0171 Georgia
[aw] Institut Universitaire de France, 1 rue Descartes, Paris, 75005 France
[ax] IN2P3, 3, Rue Michel-Ange, Paris 16, 75794 France
[ay] LPC, Campus des Cézeaux 24, avenue des Landais BP 80026, Aubière Cedex, 63171 France
[az] University of Johannesburg, Department Physics, PO Box 524, Auckland Park, 2006 South Africa
[ba] Università degli Studi della Campania "Luigi Vanvitelli", CAPACITY, Laboratorio CIRCE - Dip. Di Matematica e Fisica - Viale Carlo III di Borbone 153, San Nicola La Strada, 81020 Italy
[bb] Laboratoire Univers et Particules de Montpellier, Place Eugène Bataillon - CC 72, Montpellier Cédex 05, 34095 France
[bc] Friedrich-Alexander-Universität Erlangen-Nürnberg (FAU), Remeis Sternwarte, Sternwartstraße 7, 96049 Bamberg, Germany
[bd] Université de Haute Alsace, rue des Frères Lumière, 68093 Mulhouse Cedex, France
[be] AstroCeNT, Nicolaus Copernicus Astronomical Center, Polish Academy of Sciences, Rektorska 4, Warsaw, 00-614 Poland
[bf] UCLouvain, Centre for Cosmology, Particle Physics and Phenomenology, Chemin du Cyclotron, 2, Louvain-la-Neuve, 1349 Belgium

Acknowledgements

The authors acknowledge the financial support of the funding agencies: SC gratefully acknowledges the support from Università La Sapienza di Roma through the grant ID RM1221816813FFA3; Agence Nationale de la Recherche (contract ANR-15-CE31-0020), Centre National de la Recherche Scientifique (CNRS), Commission Européenne (FEDER fund and Marie Curie Program), LabEx UnivEarthS (ANR-10-LABX-0023 and ANR-18-IDEX-0001), Paris Île-de-France Region, France; Shota Rustaveli National Science Foundation of Georgia (SRNSFG, FR-22-13708), Georgia; The General Secretariat of Research and Innovation (GSRI), Greece Istituto Nazionale di Fisica Nucleare (INFN), Ministero dell'Università e della Ricerca (MIUR), PRIN 2017 program (Grant NAT-NET 2017W4HA7S) Italy; Ministry of Higher Education, Scientific Research and Innovation, Morocco, and the Arab Fund for Economic and Social Development, Kuwait; Nederlandse organisatie voor Wetenschappelijk Onderzoek (NWO), the Netherlands; The National Science Centre, Poland (2021/41/N/ST2/01177); The grant "AstroCeNT: Particle Astrophysics Science and Technology Centre", carried out within the International Research Agendas programme of the Foundation for Polish Science financed by the European Union under the European Regional Development Fund; National Authority for Scientific Research (ANCS), Romania; Grants PID2021-124591NB-C41, -C42, -C43 funded by MCIN/AEI/ 10.13039/501100011033 and, as appropriate, by "ERDF A way of making Europe", by the "European Union" or by the "European Union NextGenerationEU/PRTR", Programa de Planes Complementarios I+D+I (refs. ASFAE/2022/023, ASFAE/2022/014), Programa Prometeo (PROMETEO/2020/019) and GenT (refs. CIDEGENT/2018/034, /2019/043, /2020/049. /2021/23) of the Generalitat Valenciana, Junta de Andalucía (ref. SOMM17/6104/UGR, P18-FR-5057), EU: MSC program (ref. 101025085), Programa María Zambrano (Spanish Ministry of Universities, funded by the European Union, NextGenerationEU), Spain; The European Union's Horizon 2020 Research and Innovation Programme (ChETEC-INFRA - Project no. 101008324); Fonds de la Recherche Scientifique - FNRS, Belgium.